Desalination and Water Treatment
www.deswater.com

doi: 10.1080/19443994.2013.803442

52 (2014) 4305–4313
June

Taylor & Francis
Taylor & Francis Group

Hydrothermal synthesis of easy-recycled tobermorite/SiO_2/Fe_3O_4 composites for efficient treatment of phosphorus in wastewater

Shuhua Zhong[a,b,c], Huaili Sha[a,b], Yu He[a,b,*], Gongwu Song[a,b,*]

[a]*Hubei Collaborative Innovation Center for Advanced Organic Chemical Materials, Hubei University, Wuhan 430062, China*
Tel. + 862788663043; Fax: + 862788663043; email: heyu@hubu.edu.cn
[b]*Ministry of Education Key Laboratory for the Synthesis and Application of Organic Functional Molecules, Hubei University, Wuhan 430062, China*
Tel. +862788663043; Fax: +862788663043; email: songgw@hubu.edu.cn
[c]*Ezhou Municipal Environmental Protection Monitoring Station, Ezhou 436000, China*

Received 25 November 2012; Accepted 24 April 2013

ABSTRACT

In this work, tobermorite/SiO_2/Fe_3O_4 composites were designed and synthesized by hydrothermal method for the treatment of phosphorus in wastewater. The composites were characterized by scanning electron microscopy and X-ray diffraction. The removal efficiency of phosphorus on the tobermorite/SiO_2/Fe_3O_4 composites was carried out and investigated under various conditions, such as contact time, sorbent content, and pH. After the multi-run experiments, the phosphorous elimination of the tobermorite/SiO_2/Fe_3O_4 composites was declined slightly comparing with the first-run experiments. Compared with the conventional crystallization methods, tobermorite/SiO_2/Fe_3O_4 composites not only gave high efficiency to remove phosphorus from wastewater without any complicated pretreatment, but also provided excellent magnetic properties for separating the phosphorus from water, which made it easy recycled. Moreover, tobermorite/SiO_2/Fe_3O_4 composites had excellent P-elimination properties even in the strong acidic or basic conditions. Therefore, tobermorite/SiO_2/Fe_3O_4 composites were important candidate for water quality control and protection.

Keywords: Tobermorite/SiO_2/Fe_3O_4 composites; P-elimination; Easy recycled

1. Introduction

Phosphorus (P) supply (concentration and flux) is an important driver for biological activity in flowing waters and needs to be managed to avoid eutrophication impacts associated with urbanization and agricultural intensification [1]. These problems relate to human health (algal toxins), species abundance and diversity, and costs of water treatment for drinking. On the other hand, P is an essential nutrient for plants which cannot be substituted by any other element, and makes it an indispensable fertilizer component in agriculture. Therefore, the removing, recovering, and monitoring P in the water bodies are important for both large-scale environmental assessment and industrial process control. Several methods have been developed to remove phosphorus from wastewater including crystallization method, chemical precipitation method, and adsorption method [2–9]. Adsorp-

---

*Corresponding author.

1944-3994/1944-3986

tion method often applied to treat wastewater with P at low concentration (less than $1\,\mathrm{mg\,L^{-1}}$) [10,11]. Although traditional chemical precipitation method is simple and economical in operation, it has the disadvantages such as sensitivity to the environmental conditions and relatively high sludge production [12]. Crystallization process is developed to remove P from wastewater as an alternative technology. The suitable seed material in crystallization process initiates the deposition of calcium phosphate compounds onto the seed material surfaces in order to achieve equilibrium between Ca ions and phosphate [2]. Since crystallization process produced hydroxyapatite and/or magnesium ammonium phosphate crystal on the surface of granular seed crystals, it takes advantage of separating from the water and potential phosphorus recycling from the product [2]. However, several crystallization processes need an adjustment of the pH value prior to the calcium phosphate precipitation [13,14]. Therefore, it is still a challenge to explore novel, good-performance, and easy-recycled seeds for crystallization to inexpensive and facile treatment of wastewater.

Tobermorite ($Ca_5Si_6O_{18}H_2{\cdot}4H_2O$) has received much attention due to the high adsorption capacity to P and its potential applications in cation exchange and wastewater treatment [15–17]. The crystallization method based on tobermorite as the seeds was a simple technology for phosphorus recovery from wastewater, by which complex pretreatment steps as pH adjustment or CO_2 stripping can be avoided [18,19]. The major product of this crystallization process is described by Eq. (1).

$$10Ca^{2+} + 6PO_4^{2-} + 2OH^- \rightarrow Ca_{10}(OH)_2(PO_4)_6 \tag{1}$$

Although significant advances have been made in the development of tobermorite-based method for wastewater treatment, this kind of materials also encounter difficulties in easy recycling.

Herein, Tobermorite/SiO_2/Fe_3O_4 composites fabricated by hydrothermal method were employed for wastewater treatment (Fig. 1). The addition of magnetic Fe_3O_4 nanoparticles make the composite could be separated from the water by an external magnetic field [20,21]. Compared with the conventional crystallization method, Tobermorite/SiO_2/Fe_3O_4 composites not only gave high efficiency to remove P from wastewater without any complicated pretreatment, but also provided excellent magnetic properties for separating the products from water, which make it easy recycled. Moreover, Tobermorite/SiO_2/Fe_3O_4 composites had excellent P-elimination properties even in the strong acidic or basic conditions. Owing to above merits, tobermorite/SiO_2/Fe_3O_4 composites were important candidate for water quality control and protection.

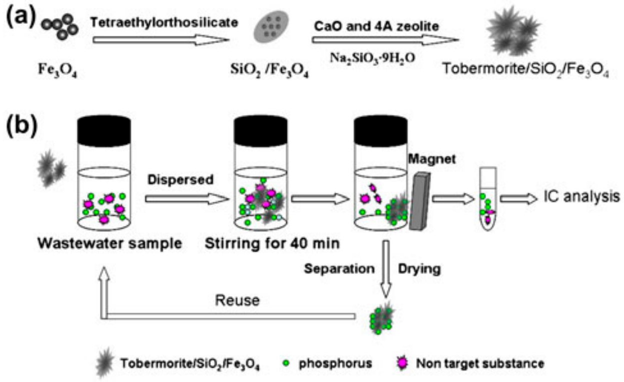

Fig. 1. Schematic diagram of tobermorite/SiO_2/Fe_3O_4 composites for P-elimination.

2. Experimental section

2.1. Chemicals and materials

All reagents used in the experiment were of analytical reagent grade. Ferric chloride ($FeCl_3{\cdot}6H_2O$) and ferrous chloride ($FeCl_2{\cdot}4H_2O$) were purchased from Tianjin Tianli Chemicals Co. (Tianjin, China). Disodium citrate ($C_6H_5O_7Na_3{\cdot}2H_2O$), tetraethyl orthosilicate (TEOS), sodium silicate ($Na_2SiO_3{\cdot}9H_2O$) were purchased from Tianjin Bodi Chemicals Co. (Tianjin, China), Aladdin chemistry Co. Ltd. (Shanghai, China) and Tianjin Kemiou Chemicals Co. (Tianjin, China), respectively.

2.2. Instruments

The crystalline structure and composition of the tobermorite/SiO_2/Fe_3O_4 composites were identified by a D/max-IIIC X-ray diffractometer (Shimadzu, Japan). The morphologies of the prepared samples were examined using JEM-100SX electron microscope (Nicolet, Japan). The oscillated treatment was by WSZ-100A air oscillation instrument (Yiheng, China). The ion chromatography (IC) analysis was performed on ICS-3000 IC (Dionex, America).

2.3. Synthesis of Fe_3O_4 and SiO_2/Fe_3O_4 nanoparticles

2.3.1. Preparation of Fe_3O_4 nanoparticles

Fe_3O_4 nanoparticles were prepared by a chemical co-precipitation method [22]. The magnetic nanoparticles were prepared based on the chemical co-precipitation of Fe^{2+} and Fe^{3+} by adding sodium hydroxide. $FeCl_2{\cdot}4H_2O$ (3.135 g, 0.0157 mol) and $FeCl_3{\cdot}6H_2O$ (8.514 g, 0.0315 mol) into 100 mL of deionized water.

After adding 12.7 mL NaOH (10 M), the reaction mixture was stirred for 1 h at room temperature. The reaction mixture was then heated to 90˚C under continuous stirring for another 1 h. 0.33 mL nitric acid was subsequently added into the reaction mixture for 0.5 h at 90˚C. Trisodium citrate (0.3 M, 50 mL) was then added, and the mixture was stirred for another 0.5 h. The reaction mixture was cooled, and ethanol was added to precipitate the iron oxides from the aqueous solutions. The mixture was purified with magnet to collect the Fe_3O_4 nanoparticles, and then removed supernatant. After repeated washing thrice, Fe_3O_4 nanoparticles were dried at 80˚C.

2.3.2. Preparation of SiO_2/Fe_3O_4 nanoparticles

The synthesized Fe_3O_4 nanoparticles were rinsed with 20 mL of anhydrous toluene twice, and then dispersed into 50 mL of anhydrous toluene. After an addition of 0.5 mL of TEOS, the mixture was sonicated for 15 min and transferred in a PTFE-lined autoclave. The autoclave was heated at 120˚C for 12 h to obtain SiO_2/Fe_3O_4 nanoparticles [23].

2.4. Preparation of tobermorite/SiO_2/Fe_3O_4 composites composites

About 0.05, 0.1, 0.15, and 0.20 g SiO_2/Fe_3O_4 nanoparticles were dispersed into pure water (25 mL), respectively, then 0.9 g of 4A zeolite powder and 1.5 g of calcium oxide was introduced into the solution under stirring. The mixture was sonicated for 30 min and then transferred into autoclaves. The autoclaves were heated for 10 h at 160˚C [24]. The synthesized tobermorite/SiO_2/Fe_3O_4 composites were coded as SAM-01, SAM-02, SAM-03, and SAM-04, respectively.

2.5. Tobermorite/SiO_2/Fe_3O_4 composites for treating wastewater

The P-concentration of simulated wastewater was 1 mg/L. The P-elimination efficiency of tobermorite/SiO_2/Fe_3O_4 composites was evaluated. 0.1 g tobermorite/SiO_2/Fe_3O_4 composites were added into 10 mL solution with 1 mg/L P to oscillate on the air oscillation instrument for 40 min, and then the mixture was separated with the magnet.

2.6. IC analysis

The IC was employed to determine phosphorus (as phosphate) of the supernatant. Five preparations were typically made gravimetrically each for the calibration standard. The mass fraction of phosphate in these solutions ranged from 0.5 to 15 mg/L. After filtrating with 0.22 μm filter membrane for pre-treatment, the P-concentration of the supernatant was determined by IC analysis. The operation conditions of IC were displayed in Table 1.

Table 1
IC operating conditions of ICS-3000 for analysis of phosphate

Column	Dionex ionpac AS11-HC, analytical (250 mm × 2 mm)
Guard column	Dionex ionpac PA-10 (2 × 50 mm)
Temperature	Column set at 30˚C, Cell set at 35˚C
Detection	Suppressed Conductivity, Temperature compensation, 1.7˚C^{-1}
Suppressor	Anion self-regenerating suppressor (ASRS 300 2 mm) auto suppression recycle mode
Eluent	30 mM KOH
Flow rate	0.38 mL/min
Applied current	29 mA
Injection volume	2.5 μL
Data collection rate	5.0 Hz
Quantification	Peak area
Analyte retention time	8.25 min

3. Results and discussion

3.1. Synthesis and characterization of tobermorite/SiO_2/Fe_3O_4 composites

Fe_3O_4 nanoparticles were prepared by a chemical co-precipitation method [22]. Then, the Fe_3O_4 nanoparticles were modified by SiO_2 [23]. Figs. 2 and 3

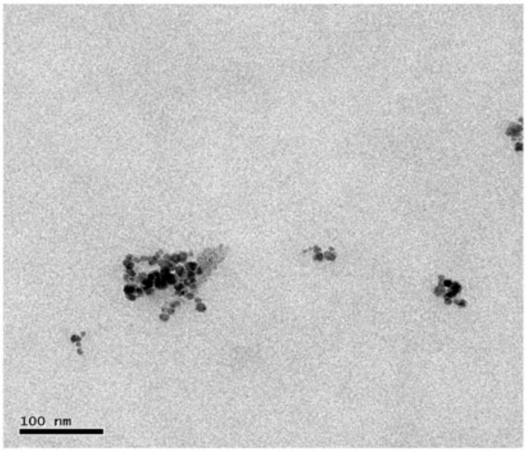

Fig. 2. TEM image of Fe_3O_4 nanoparticles.

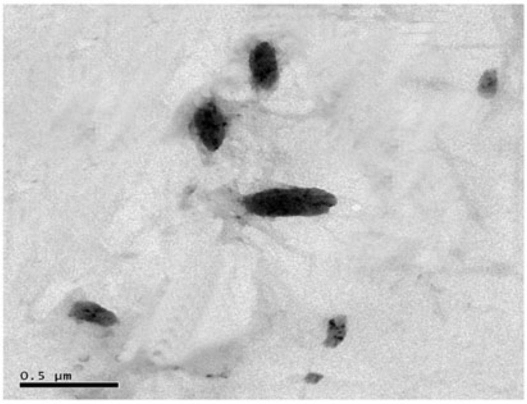

Fig. 3. TEM image of SiO_2/Fe_3O_4 nanoparticles.

show the transmission electron microscopy (TEM) image of Fe_3O_4 and SiO_2/Fe_3O_4 nanoparticles. The Fe_3O_4 nanoparticles were spherical with a particle size of about 5 nm (Fig. 2), while SiO_2/Fe_3O_4 nanoparticles were spindle in shape with several Fe_3O_4 nanoparticles as the core (Fig. 3). Fig. 4 shows the XRD pattern of Fe_3O_4. The intense diffraction peaks indexed to (2 2 0), (3 1 1), (4 0 0), (4 2 2), (5 1 1), and (4 4 0) planes appearing at $2\theta = 30.15$, 36.27, 43.32, 53.89, 57.13, and 62.29°, respectively, are consistent with the standard XRD data for the cubic phase Fe_3O_4 with a face-centered cubic structure.

The tobermorite/SiO_2/Fe_3O_4 composites were synthesized by hydrothermal method [24]. To observe the effect of Fe_3O_4 nanoparticles content in the hybrid materials, we synthesized the tobermorite/SiO_2/Fe_3O_4 composites by using different weight ratio of SiO_2/Fe_3O_4 nanoparticles to tobermorite (0.05:1.5, 0.1:1, 0.15:1.5, and 0.2:1.5). The XRD pattern is often used as a measure of product yield [25,26]. XRD patterns of SAM-01, SAM-02, SAM-03, SAM-04, and SiO_2/Fe_3O_4 nanoparticles are shown in Fig. 5. Fig. 5 shows that the diffraction peak of pure tobermorite ($2\theta = 7°, 30°$; JCPDS No.19-1364) SiO_2/Fe_3O_4 nanoparticles ($2\theta = 36°, 53°, 64°$; JCPDS No.16-629) still appeared in tobermorite/SiO_2/Fe_3O_4 composites. Evaluated from the XRD peak intensity, the mean percentage content of tobermorite in SAM-02 is highest in these four samples. The synthesized tobermorite/SiO_2/Fe_3O_4 composites SAM-01, SAM-02, SAM-03, and SAM-04 were applied for treating phosphorus and the results were shown in Fig. 6. Fig. 6 demonstrated the synthesized sample SAM-02 had the highest P-elimination efficiency, which was in consistent with the results of XRD.

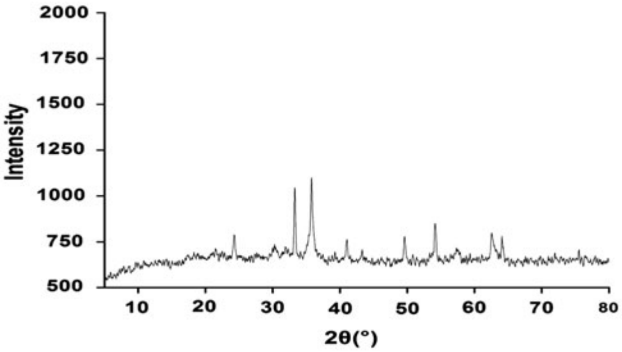

Fig. 4. The XRD pattern of Fe_3O_4.

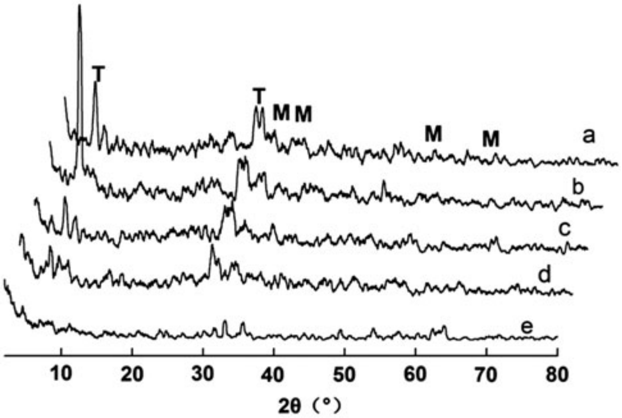

Fig. 5. XRD results of the synthesized tobermorite/SiO_2/Fe_3O_4 composites using different weight ratio of SiO_2/Fe_3O_4 nanoparticles to tobermorite. SAM-01 (a), SAM-02 (b), SAM-03 (c), SAM-04 (d), and SiO_2/Fe_3O_4 nanoparticles (e). (T) Tobermorite, (M) SiO_2/Fe_3O_4 nanoparticles.

The VSM picture in Fig. 7 demonstrated that it can be separated by an external applied magnetic field from wastewater. The magnetization property of as-prepared tobermorite/SiO_2/Fe_3O_4 composites was investigated at room temperature by measuring the magnetization curve (Fig. 7). The saturation magnetization of the composite was $3.5\,\mathrm{emu g^{-1}}$ which indicated that the tobermorite/SiO_2/Fe_3O_4 composites could be applied for magnetic separation.

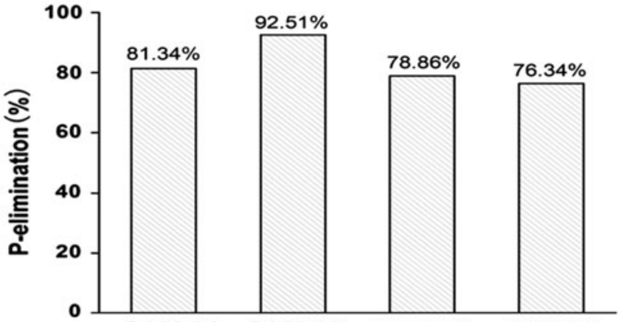

Fig. 6. The P-elimination of different tobermorite/SiO_2/Fe_3O_4 composites.

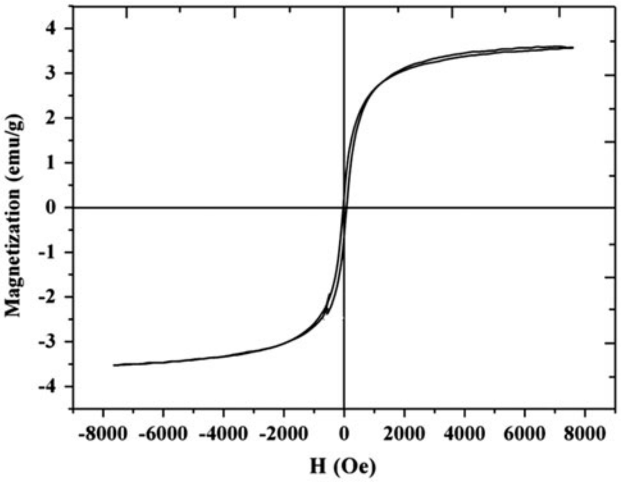

Fig. 7. The VSM picture of tobermorite/SiO_2/Fe_3O_4 composites.

The morphology of the tobermorite and tobermorite/SiO_2/Fe_3O_4 composites was verified by scanning electron microscopy (SEM). The graph shows pure tobermorite was needle-shaped crystal (Fig. 8(d)). After doped with SiO_2/Fe_3O_4 nanoparticles, tobermorite/SiO_2/Fe_3O_4 composites exhibited needle-shaped crystals with some twine shape around (Fig. 8(a, b, c)).

The surface conditions of tobermorite/SiO_2/Fe_3O_4 composites before and after used for P-elimination was also compared by SEM (Fig. 9). Before adsorption of phosphorus, the fine cardhouse structure with needlelike crystals on the surface of composites could be observed (Fig. 9(a)). However, after adsorption the crystal line form disappeared from the SEM photograph (Fig. 9(b)). Hence, the P-elimination process seemed to chemisorb tobermorite with twine around its needle-like crystal.

3.2. *Influence of the oscillation time*

In the proposed method, oscillation time was an important parameter affecting the P-elimination efficiency of tobermorite/SiO_2/Fe_3O_4 composites to wastewater. The effect of oscillation time on P-elimination efficiency was evaluated and the results were shown in Fig. 10. The P-elimination efficiency increased with increment of oscillation time and then approach a stable value after oscillation over 30 min. Therefore, 40 min was chosen for further the experiment.

3.3. *The best dosage of tobermorite/SiO_2/Fe_3O_4 composites in the P-elimination process*

The dosage of tobermorite/SiO_2/Fe_3O_4 composites were one of the key kinetic factors of P-elimination process. To investigate the effect of the dosage of tobermorite/SiO_2/Fe_3O_4 composites on the P-elimination process, a series of P-elimination experiments were carried out by varying the amount of tobermorite/SiO_2/Fe_3O_4 composites from 0.5 to 20 g l^{-1}. The changed P-elimination efficiency with various

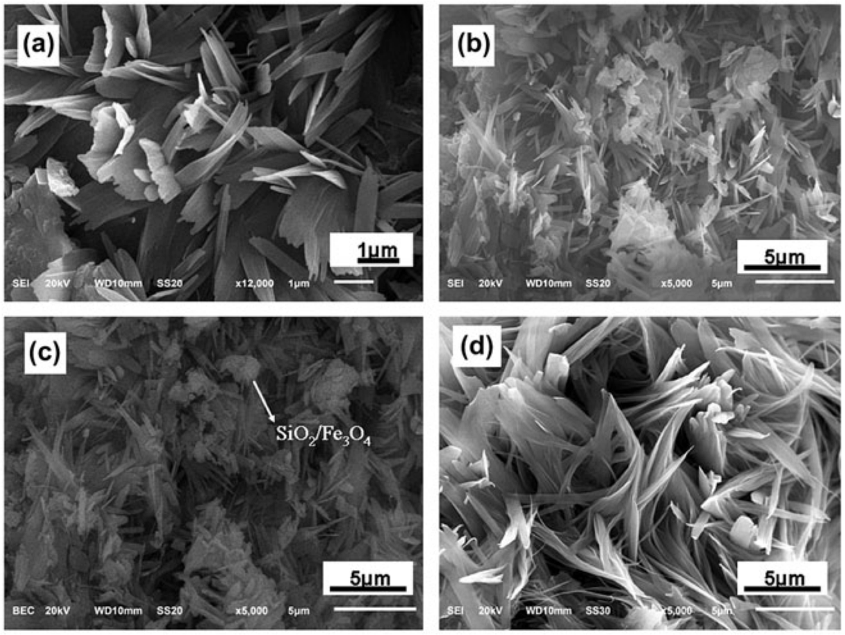

Fig. 8. SEM images of the synthesized tobermorite/SiO_2/Fe_3O_4 composites (a, b, c) and tobermorite (d).

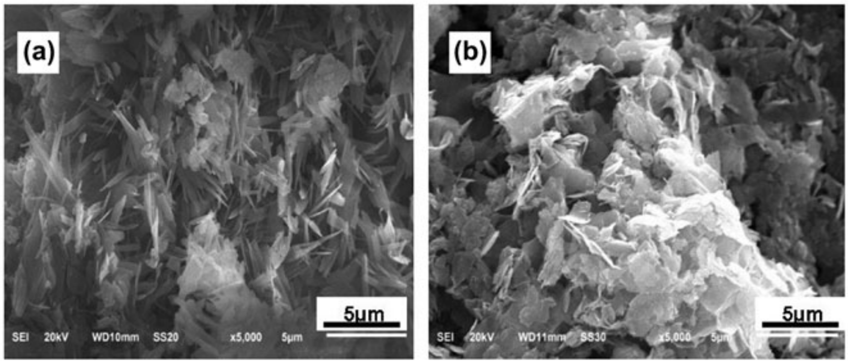

Fig. 9. SEM images of the synthesized tobermorite/SiO_2/Fe_3O_4 composites before (a) and after (b) used.

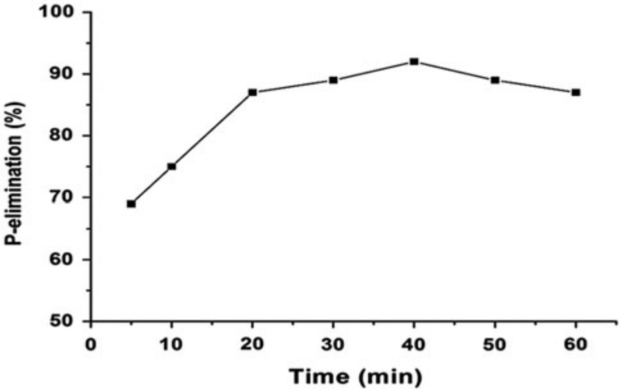

Fig. 10. The effect of oscillation time on P-elimination efficiency of tobermorite/SiO_2/Fe_3O_4 composites.

tobermorite/SiO_2/Fe_3O_4 composites dosages is shown in Fig. 11. The P-elimination efficiency increased when the concentration of tobermorite/SiO_2/Fe_3O_4 composites was from 0.5 to $10\,g\,l^{-1}$, and then approached a stable value with the further increased concentration of tobermorite/SiO_2/Fe_3O_4 composites. Therefore, $10\,g\,l^{-1}$ tobermorite/SiO_2/Fe_3O_4 composites were chosen for further experiment.

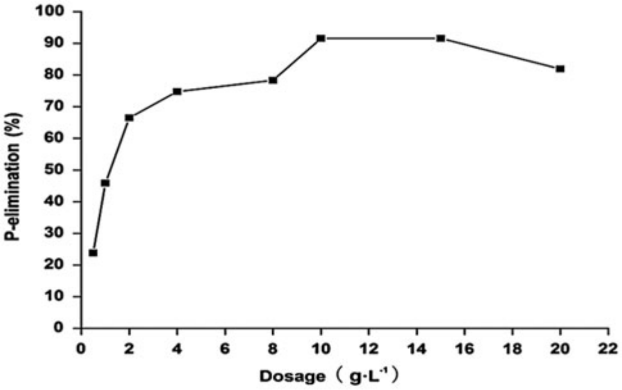

Fig. 11. The P-elimination of different dosage of tobermorite/SiO_2/Fe_3O_4 composites composites.

3.4. Effect of pH on P-elimination process

The pH of aquatic environment played an important role on the P-elimination efficiency of the crystallization methods, since the crystallization of calcium phosphate compounds were influence by pH [18,19]. The effect of pH range 1.8–13 on the P-elimination process of tobermorite/SiO_2/Fe_3O_4 composites is shown in Fig. 12. Fig. 12 shows that tobermorite/SiO_2/Fe_3O_4 composites had excellent P-elimination properties even in the strong acidic or basic conditions. This system could overcome the disadvantages of pH-sensitive in the conventional crystallization methods.

3.5. The durability of the tobermorite/SiO_2/Fe_3O_4 composites

In order to avoid environmental pollution and meet the need of stringent ecological and economic demands

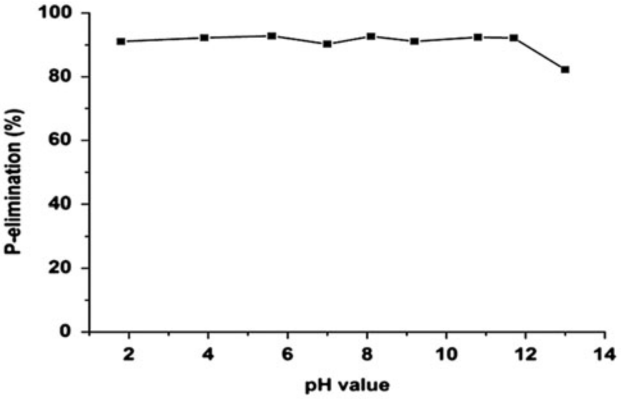

Fig. 12. The P-elimination of tobermorite/SiO_2/Fe_3O_4 composites in different pH.

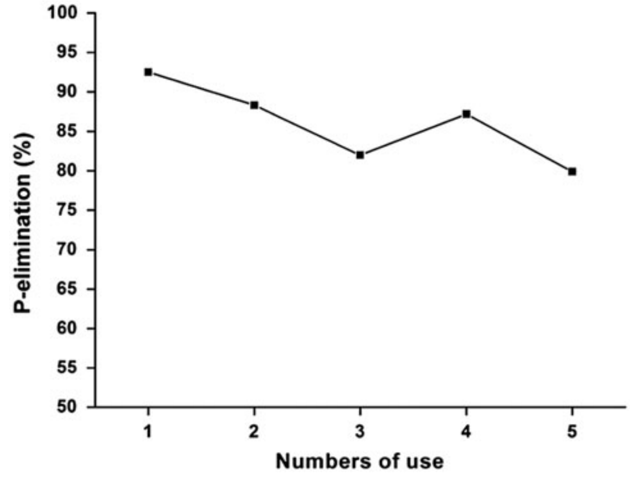

Fig. 13. The durability of the tobermorite/SiO_2/Fe_3O_4 composites.

for sustainability, the regeneration and reuse of tobermorite/SiO_2/Fe_3O_4 composites were of particular importance. The durability of the tobermorite/SiO_2/Fe_3O_4 composites was evaluated by P-elimination performance of the reused tobermorite/SiO_2/Fe_3O_4 composites on the $1\,\mathrm{mg\,l^{-1}}$ phosphorous solution (Fig. 13). After the multi-run experiments, the P-elimination performance of the reused tobermorite/SiO_2/Fe_3O_4 composites was still higher than 80%, which shows satisfactory stability of the P-elimination performance. Although the tobermorite/SiO_2/Fe_3O_4 composites may lose some tobermorite from the long-term use, it is possible to restore the tobermorite/SiO_2/Fe_3O_4 composites by repeating the tobermorite coating process for the recovery of the P-elimination performance.

3.6. The application of tobermorite/SiO_2/Fe_3O_4 composites for P-elimination in real samples

In order to evaluate the practicability of the developed method, the tobermorite/SiO_2/Fe_3O_4 composites were utilized for P-elimination in three real samples under selected conditions. The results showed that these real samples had little interference with the performance of tobermorite/SiO_2/Fe_3O_4 composites, suggesting that this new method was suitable for the removal of phosphorus from wastewater (Fig. 14 and Table 2). In addition, tobermorite/SiO_2/Fe_3O_4 composites also showed excellent P-elimination efficiency for industrial wastewater, suggesting that the as-proposed method should be a general one for the removal of P pollutants. The P-elimination of tobermorite and tobermorite/SiO_2/Fe_3O_4 composites is also compared in Fig. 15. The tobermorite and tobermorite/SiO_2/Fe_3O_4 composites had the same P-elimination effect for the wastewater indicating no synergetic effects between tobermorite and SiO_2/Fe_3O_4 for the P elimination.

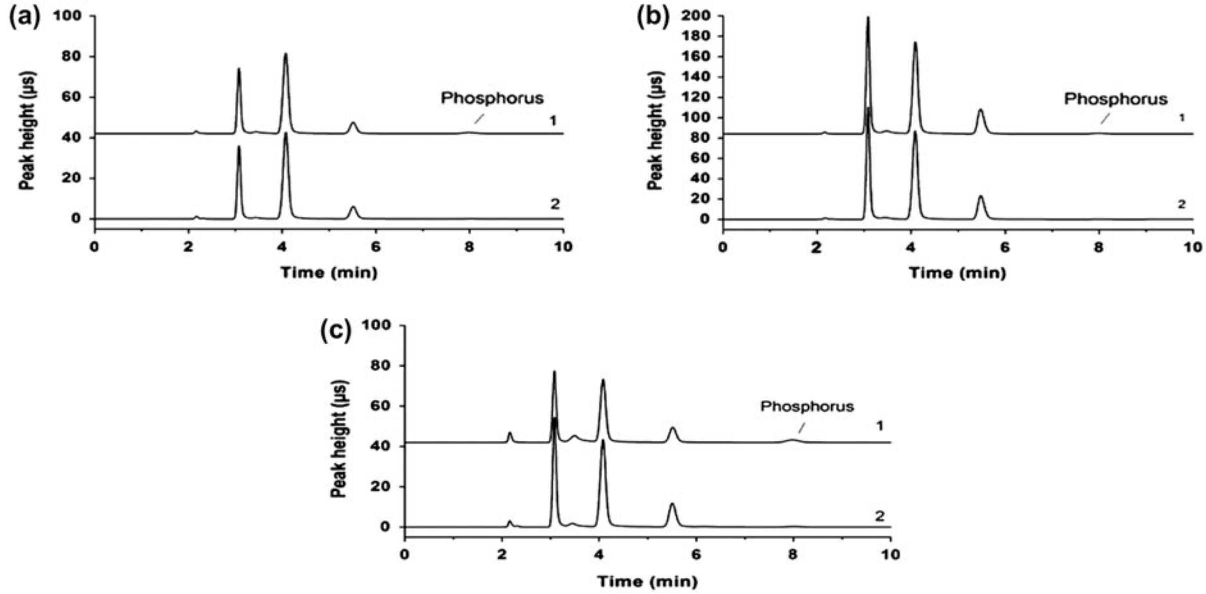

Fig. 14. The ion chromatogram of real samples before (1) and after (2) treated by the tobermorite/SiO_2/Fe_3O_4 composites. Running water spiked phosphorus at concentration of 0.76 mg/L (a), Shahu Lake (b), wastewater from Huangmailing factory (c).

Table 2
Parameters of P-elimination by the proposed method

Sample	C_0 (mg/L)	C_1 (mg/L)	P-elimination (%)	RSD (%)
Running water	0.76	0.16	78.95	3.8
ShaHu Lake	0.75	0.15	80.00	3.7
Wastewater	1.53	0.36	76.47	4.2

C_0 was the original P-concentration of the sample.
C_1 was the P-concentration of the sample after treated.
The running water was spiked with phosphorus at concentration of 0.76 mg/L.
The wastewater, from Hubei provincial Huangmailing phosphate Chemical Co. Ltd., has been diluted 1000×.

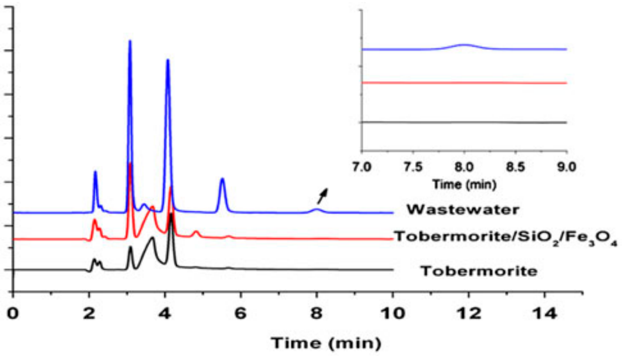

Fig. 15. The ion chromatogram of wastewater before and after treated by the tobermorite and tobermorite/SiO_2/Fe_3O_4 composites.

4. Conclusions

In this work, we explored the rapid, versatile, and economical method for P-elimination in wastewater based on tobermorite/SiO_2/Fe_3O_4 composites with high P-elimination efficiency and separation ability. The feasibility and performance of the tobermorite/SiO_2/Fe_3O_4 composites for P-elimination were evaluated by IC. Compared with traditional P-elimination materials, tobermorite/SiO_2/Fe_3O_4 composites can be collected easily and rapidly with a magnet in the adsorption process. Besides, its adsorption properties were independent of the solution pH. This research provides the advanced tobermorite/Fe_3O_4 composites for monitoring and control of phosphorus.

Acknowledgments

This work was financially supported by the Scientific Research Foundation of Education Commission of Hubei Province (Q20111010 and T201101), the Natural Science Foundation of Hubei Province (2011CDB059 and 2011CDA111), the foundation of Engineering Research Center of Nano-Geomaterials of Ministry of Education (GUGNGM201207) and Research Fund for the Doctoral Program of Higher Education of China (20114208120006).

References

[1] P.J.A. Wither, H.P. Jarvie, Delivery and cycling of phosphorus in rivers: A review, Sci. Total Environ. 400 (2008) 379–395.
[2] H. Jang, S.H. Kang, Phosphorus removal using cow bone in hydroxyapatite crystallization, Water Res. 36 (2002) 1324–1330.
[3] P. Battistoni, A. DeAngelis, M. Prisciandaro, R. Boccadoro, D. Bolzonella, Phosphorus removal from anaerobic supernatants by struvite crystallization: Long term validation and process modeling, Water Res. 36 (2002) 1927–1938.
[4] A. Genza, A.K. Üllerb, M. Jekel, Advanced phosphorus removal from membrane filtrates by adsorption on activated aluminium oxide and granulated ferric hydroxide, Water Res. 38 (2004) 3523–3530.
[5] G.M. Ayoub, B. Koopman, N. Pandya, Iron and aluminum hydroxy (oxide) coated filter media for low-concentration phosphorus removal, Water Environ. Res. 73 (2001) 478–485.
[6] D.J. Akhurst, G.B. Jones, M. Clark, D. McConchie, Phosphate removal from aqueous solutions using neutralised bauxite refinery residues (Bauxsol™), Environ. Chem. 3 (2006) 65–74.
[7] W.W. Huang, S.B. Wang, Z.H. Zhu, L. Li, X.D. Yao, V. Rudolph, F. Haghseresht, Phosphate removal from wastewater using red mud, J. Hazard. Mater. 158 (2008) 35–42.
[8] S.G. Lu, S.Q. Bai, L. Zhu, H.D. Shan, Removal mechanism of phosphate from aqueous solution by fly ash, J. Hazard. Mater. 161 (2009) 95–101.
[9] A. Ugurlu, B. Salman, Phosphorus removal by fly ash, Environ. Int. 24 (1998) 911–918.
[10] S. Tanada, M. Kabayama, N. Kawasaki, T. Sakiyama, T. Nakamura, M. Araki, T. Tamura, Removal of phosphate by aluminum oxide hydroxide, J. Colloid Interface Sci. 257 (2003) 135–140.
[11] L. Zeng, X.M. Li, J.D. Liu, Adsorptive removal of phosphate from aqueous solutions using iron oxide tailings, Water Res. 38 (2004) 1318–1326.
[12] F. Haghseresht, S.B. Wang, D.D. Do, A novel lanthanum-modified bentonite, Phoslock, for phosphate removal from wastewaters, Appl. Clay Sci. 46 (2009) 369–375.
[13] D. Donnert, M. Salecker, Elimination of phosphorus from waste water by crystallisation, Environ. Technol. 20 (1999) 735–742.
[14] A. Giesen, Crystallisation process enables environmental friendly phosphate removal at low costs, Environ. Technol. 20 (1999) 769–776.
[15] S. Komarneni, D.M. Roy, Tobermorites: A new family of cation exchangers, Science 221 (1983) 647–648.
[16] S. Kaneco, K. Itoh, H. Katsumata, T. Suzuki, K. Masuyama, K. Funasaka, K. Hatano, K. Ohta, Removal of natural organic polyelectrolytes by adsorption onto tobermorite, Environ. Sci. Technol. 37 (2003) 1448–1451.
[17] H. Maeda, K. Ioku, E.H. Ishida, Hydrothermal synthesis of tobermorite/hydroxyapatite composites, Mater. Lett. 62 (2008) 3291–3293.
[18] U. Berg, D. Donnert, P.G. Weidler, E. Kaschka, G. Knoll, R. Nüesch, Phosphorus removal and recovery from wastewater by tobermorite-seeded crystallisation of calcium phosphate, Water Sci. Technol. 53 (2006) 131–138.

[19] E.H. Kim, S.B. Yim, H.C. Jung, E.J. Lee, Hydroxyapatite crystallization from a highly concentrated phosphate solution using powdered converter slag as a seed material, J. Hazard. Mater. 136 (2006) 690–697.

[20] Z. Liu, J. Ding, J. Xue, A new family of biocompatible and stable magnetic nanoparticles: Silica cross-linked pluronic F127 micelles loaded with iron oxides, New J. Chem. 33 (2009) 88–92.

[21] N. Shrestha, J. Macak, F. Schmidt-Stein, R. Hahn, C. Mierke, B. Fabry, P. Schmuki, Magnetically guided titania nanotubes for site-selective photocatalysis and drug release, Angew. Chem. Int. Ed. 48 (2009) 969–972.

[22] Y.M. Yang, J.X. Aw, K. Chen, F. Liu, P. Padmanabhan, Y. Long, H.Z. Cheng, B.G. Xin, Enzyme-responsive multifunctional magnetic nanoparticles for tumor intracellular drug delivery and imaging, Chem. Asian J. 6 (2011) 1381–1389.

[23] S.X. Zhang, H.Y. Niu, Y.Q.Y. Cai, A.L. Shi, Barium alginate caged Fe_3O_4/C_{18} magnetic nanoparticles for the pre-concentration of polycyclic aromatic hydrocarbons and phthalate esters from environmental water samples, Anal. Chim. Acta 665 (2010) 167–175.

[24] Y. Wei, R. Yang, Y.X. Zhang, L. Wang, J.H. Liu, X.J. Huang, High adsorptive γ-AlOOH(boehmite)/SiO_2/Fe_3O_4 porous magnetic microspheres for detection of toxic metal ions in drinking water, Chem. Commun. 47 (2011) 11062–11064.

[25] H.C. Hu, W.H. Chen, T.Y. Lee, Synthesis kinetics and particle size distribution of zeolite A, J. Cryst. Growth 108 (1991) 561–571.

[26] N. Shigemoto, S. Sugiyama, H. Hayashi, K. Miyaura, Scanning electron microscopic observation during crystallization of Na-X and related zeolites compared with X-ray diffraction crystallinity, J. Mater. Sci. Lett. 13 (1994) 660–662.